

## Monte Carlo Simulation Studies of Conformational Properties of Polyelectrolytes with Maleic Acid Units

Yuji HIROSE, Minoru ONODERA, Seigou KAWAGUCHI,\* and Koichi ITO\*

*Department of Materials Science, Toyohashi University of Technology,  
Tempaku-cho, Toyohashi 441, Japan*

(Received November 8, 1994)

**ABSTRACT:** Conformational properties of polyelectrolyte chain with maleic acid units (MA polyelectrolyte) are investigated by a mean of Monte Carlo simulation. The polyelectrolyte chains are modeled as a self-avoiding walk on tetrahedral lattice with charges fixed. The each charge interacts through Debye–Hückel potential and attraction energy from hydrogen bonding between un-ionized and ionized carboxyl groups in short-range. Mean-square end-to-end distance,  $\langle R^2 \rangle$ , mean-square radius of gyration,  $\langle S^2 \rangle$ , and mean conformational energy,  $\langle E \rangle$ , are simulated as a function of degree of polymerization ( $N$ ) and dissociation ( $\alpha$ ), and salt concentration ( $C_s$ ). The dependence of  $\langle R^2 \rangle$  and  $\langle S^2 \rangle$  on  $N$  shows that MA polyelectrolyte chain assumes a rod like conformation at high  $\alpha$  and low  $C_s$ . The simulation results provide an interpretation for characteristic viscometric behavior of MA polyelectrolytes which show a maximum in an intrinsic viscosity nearly at  $\alpha=0.5$ . The polymer dimensions in the region of  $\alpha \leq 0.5$  increases with the energy of the hydrogen bonding assumed. The characteristic viscometric behavior of MA polyelectrolytes is deduced to result from the balance between repulsion from the electrostatic interaction and attraction from the hydrogen bonding in short-range.

**KEY WORDS** Monte Carlo Simulation / Conformation / Hydrogen Bond / Polyelectrolyte / Intrinsic Viscosity / Radius of Gyration / Dielectric Constant /

Solution properties of macromolecules strongly depend on conformation of a polymer chain. The conformational properties of an un-charged polymer chain have been fairly understood by much theoretical, numerical, and experimental effort.<sup>1,2</sup> In contrast, the understanding of the conformation for a polyelectrolyte chain still remains many unanswered subjects. The difficulty in describing behavior of the polyelectrolyte solutions comes from electrostatic interaction among dense charges fixed on the polymer backbone, which depends on density and distribution of the charges of the polyelectrolyte, as well as solvent property.<sup>3,4</sup>

The conformational properties of un-charged polymer is normally determined in

terms of short- and long-range interactions.<sup>1</sup> The former is related to chain stiffness, persistence length of the polymer, Kuhn segment length, and the latter, to the excluded volume. This also holds for the conformational properties of polyelectrolyte chains. The investigation is, however, rather complicated because the electrostatic interaction affects concurrently on both short- and long-range in the polyelectrolyte chain. Two interpretations for the polyelectrolyte conformation have been established. One is the increase of electrostatic persistence length ( $L_e$ ) with increasing the electrostatic interaction for wormlike chain.<sup>5,6</sup> The total persistence length ( $L_t$ ) of the polyelectrolyte chain is expressed by the sum of intrinsic persistence length ( $L_0$ ) and  $L_e$ .

\* To whom correspondence should be addressed.

Other is an electrostatic excluded volume.<sup>7,8</sup> The great contributions for the conformation of vinylic polyelectrolyte chain have been done by Nagasawa and co-workers.<sup>9</sup> The several experimental results including intrinsic viscosity, light, and small-angle X-ray scattering, concluded that the conformation of vinylic polyelectrolyte chain is primarily determined by the long-range electrostatic interaction at least salt concentration ( $C_s$ )  $> 0.01 N$ .

On the other hand, the solution behavior of the polyelectrolyte chains in a salt-free solution is radically different from that in added salt solution. The difference is very strikingly revealed in the studies of the dependence of viscosity on polymer concentration ( $C_p$ ) in the absence and presence of low-molecular-weight salts. In the former case, the dilution produces continuous changes in the nature of the electrostatic environments of individual polyions, leading to large changes in both intra- and inter-polyion interactions.<sup>10</sup> These changes result in characteristic viscosity curves different from that for nonionic polymers. Once the salts are added, the viscosity is remarkably depressed, and the concentration dependence of the reduced viscosity ( $\eta_{sp}/C_p$ ) is quite reminiscent of that obtained in the solutions of the nonionic polymers. The simple electrolyte serves to stabilize the electrostatic environments around the polyions, thus suppressing changes in polyion dimensions and polyion-polyion interactions.

We have reported in the previous papers<sup>11</sup> that an alternating copolymer of isobutylene with maleic acid (PIM), poly(maleic acid) (PMA), and its stereoisomer, poly(fumaric acid) (PFA), dissociate apparently in two steps at a half degree of dissociation ( $\alpha$ ). PMA and PFA have charge densities exactly twice as high as a conventional vinylic carboxylic polyacid, poly(acrylic acid) (PAA). PIM has the same average charge density as PAA but two carboxyl groups of which reside locally closer to each other as a pair. Theoretical studies on the potentiometric titration concluded that

strong short-range electrostatic interaction plays a dominant role in their dissociation behavior.<sup>11b,c</sup>

The viscometric behavior was also quietly characteristic in these polyelectrolytes solutions, when compared to that of PAA. The intrinsic viscosity,  $[\eta]$ , showed a maximum nearly in the vicinity of  $\alpha = 0.5$ . This seems to be an inherent behavior of the polyelectrolytes with maleic acid units (MA polyelectrolyte). The pioneering works by Strauss *et al.*<sup>12</sup> and Sugai *et al.*<sup>13</sup> who studied the solution properties of alternating copolymers of hydrophobic vinylic monomer with maleic acid, should be noted, but their primary concerns were focused on the conformational transition from compact to extended coil. The decrease of  $[\eta]$  with  $\alpha$  in the region of  $\alpha > 0.5$  can not be explained by the current theories. Two possible reasons for this behavior are increase of local salt concentration near MA polyelectrolyte chain and formation of hydrogen bonding between un-ionized and ionized carboxyl groups. The former is likely in the polyelectrolytes with high charge density. According to Manning's ion condensation theory,<sup>14</sup> counterion condensation begins to take place at  $\alpha = 0.16$  for PMA, and 0.32 for PIM and PAA. This clearly results in the decrease of net chain expansion throughout the decrease both of short- and long-range electrostatic interaction. In the latter, we have confirmed the existence of intramolecular hydrogen bonding between ionized and nearest neighboring un-ionized carboxyl groups in these polyelectrolytes.<sup>11</sup> Such a short-range intramolecular hydrogen bonding is reasonably thought to affect on a flexibility of the polymer chain through the depression of free rotation. Therefore, we wished to investigate how the hydrogen bonding affects global conformation of the polyelectrolyte chain. In this paper, Monte Carlo simulation method with the effect of hydrogen bonding has been developed and investigated the chain conformation of the MA polyelectrolytes.

Much effort has been devoted to study Monte Carlo simulations for polymer systems.<sup>15,16</sup> The computer simulation provides a direct information about the conformational properties of polymers. The simulations for un-charged polymers have been extensively studied by Monte Carlo method and molecular dynamic method. Past several years, Monte Carlo method has been applied to study the conformational properties of polyelectrolyte chains. Key contributions have been made by the groups of Brender *et al.*,<sup>17</sup> Prausnitz *et al.*,<sup>18</sup> and Christos *et al.*<sup>19,20</sup>

In this paper, we report Monte Carlo simulation studies for PMA and PAA polyelectrolyte chains. Especially, we focus on the influences of neutralization and short-range hydrogen bonding on the global conformation. The polymer chains are modeled as a self-avoiding walk on *tetrahedral lattice*. In addition, to estimate the effect of hydrogen bond quasi-configuration of the carboxyl groups are incorporated to the present model. The factors which affect on the conformation are charge density, salt concentration, and hydrogen bonding. The each charge interacts through Debye–Hückel potential and attractive force from hydrogen bonding. Therefore, this work provides the effect of competition between coulombic and attractive interaction on the conformational properties.

## SIMULATION METHOD

### Model Description

The polyelectrolyte chain is represented as a self-avoiding walk (SAW) of  $N-1$  steps ( $N$  segments) on tetrahedral lattice, as shown in Figure 1. The bond length is  $1.54 \text{ \AA}$ . Some charges are placed on a lattice in order to model the partially neutralized polyelectrolyte chain. PMA has the carboxylic acid groups on every carbon atom in a backbone. Fully ionized chains of PMA and PFA, therefore, are represented as a lattice chain with charges on every bead. The degree of dissociation ( $\alpha$ ) is

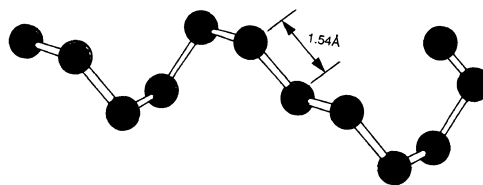


**Figure 1.** A representative picture of the tetrahedral lattice chain. The bond length is  $1.54 \text{ \AA}$ . The picture is drawn by “Ball and Stick” model.

defined

$$\alpha = \frac{Q}{Q + Q_0} \quad (1)$$

where  $Q$  and  $Q_0$  are the number of ionized beads and un-ionized ionizable beads, respectively. The lattice chain for PMA at  $\alpha=0.5$  corresponds to that for PAA chains at  $\alpha=1.0$ , where the charges are fixed alternatively along the chain. For the position of these charges, the symmetry for the location of charged beads with respect to the center of the chain is assumed in the region of  $0 < \alpha \leq 0.5$ . Obviously, we can see that the system we use does not need the periodic boundary condition.

The detailed nature of the ionic atmosphere around a polyion is not considered in the present study. Each charged bead interacts with every other charged beads via a Debye–Hückel potential,

$$u_{ij} = \frac{z_i z_j e^2}{4\pi\epsilon_0 \epsilon_r r_{ij}} \exp[-\kappa r_{ij}] \quad (2)$$

where  $u_{ij}$  is the potential energy between  $i$ - and  $j$ -th beads on a chain,  $r_{ij}$  is the distance between  $i$ - and  $j$ -th bead,  $z_i$  and  $z_j$  are the valence of the bead  $i$  and  $j$ ,  $e$ , an elementary electric charge,  $\epsilon_0$ , the permittivity of vacuum, and  $\epsilon_r$ , the relative dielectric constant of the solvent, 78 at  $25^\circ\text{C}$ .  $\kappa$  is the Debye–Hückel parameter which is given by

$$\kappa^2 = \frac{e^2 N_A}{\epsilon_0 \epsilon_r k T} \sum_i C_i \quad (3)$$

where  $N_A$  is Avogadro’s constant,  $k$ , Boltz-

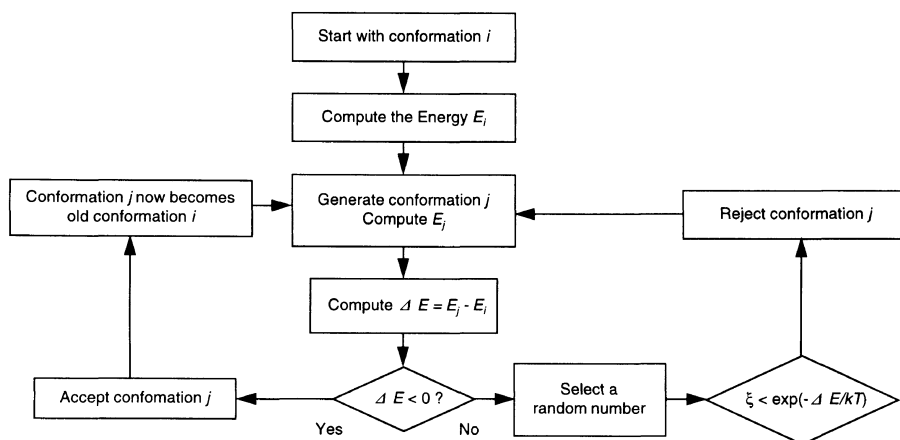


Figure 2. A flow chart of the present calculation. The symbols are explained in the text.

mann constant,  $T$ , absolute temperature, and  $C_i$ , the concentration of ionic species  $i$ . The counterions from polyelectrolyte are neglected in this study. The torsional potential based on steric hindrance is also not incorporated. The tetrahedral lattice mimics the actual chemical geometry of polyelectrolyte chain to the lattice chain.

The conformational energy per a chain,  $E_s$ , at certain conformation,  $s$ , is given by the sum of the potential  $u_{ij}$  between all bead pairs.

$$E_s = \sum_{i=1}^{N-1} \sum_{j=i+1}^N u_{ij} \quad (4)$$

#### Simulation Procedure

We have performed a Monte Carlo simulation according to Metropolis' sampling procedure<sup>21</sup> to obtain ensemble-average chain properties of an isolated polyelectrolyte chain. The procedure of the present simulation is presented in Figure 2. The chain motion is performed by "reptation motion" method,<sup>19</sup> as shown in Figure 3. In this movement, one end of the chain is chosen randomly, say "tail", and the other end is designated as the "head". A new bead position is generated and attached to the head in such a way as to satisfy the constraints of fixed bond angle and bond length. These motions we consider are repeated to sample over the conformational space of the

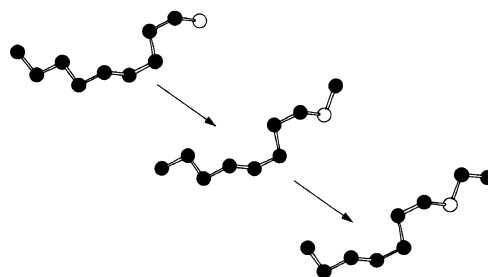


Figure 3. The representative figure for the reptation motion.

polyelectrolyte.

Trial chain conformations are accepted on the basis of the following probability,

$$P_{s+1} = \min \left[ 1, \exp \left( -\frac{\Delta E}{kT} \right) \right] \quad (5)$$

where  $\Delta E$  is the energy change in going from conformation  $s$  to conformation  $s+1$  ( $\Delta E = E_{s+1} - E_s$ ). When  $\Delta E < 0$ , the moving is always accepted and the moving is tried. When  $\Delta E > 0$ , the moving is accepted with the probability of  $\exp(-\Delta E/kT)$ . If the conformation  $s+1$  is rejected, the previous conformation is kept and the next moving is tried. We use a SAW chain as an initial conformation of polyelectrolyte chain. It is confirmed that the property of the initial chain conformation is not important since its conformation is forgotten by proceed-

ing the reptation moves.  $N^2$  reptation motion cycles are required to generate a new conformation to avoid the correlation between the successive conformations. We use the method proposed by Christos *et al.*<sup>20</sup> That is, the simulation is divided into blocks of the order of  $N^2$  conformations (number of block cycles). All the simulation results are obtained by "stroboscopic" averaging. After discarding the first few blocks to allow the chain to attain an equilibrium conformation, the statistical chain properties are calculated by averaging each property over the conformations in each block of the data. One hundred to five hundreds blocks are required to terminate a simulation calculation. In this way, we simulate a polyelectrolyte chain.

#### Effect of Hydrogen Bonding

As mentioned in Introduction, we confirmed in the previous works<sup>11</sup> the formation of intramolecular hydrogen bond between un-ionized and ionized carboxyl groups in the MA polyelectrolyte solutions by means of FT-IR and UV spectroscopies. Therefore, the effect of short-range intramolecular hydrogen bond on the global properties is examined. The several assumptions are made for the model including the hydrogen bond formation:

(1) The intramolecular hydrogen bond is formed only between an ionized and the nearest neighboring un-ionized beads.

(2) The tacticity for PMA chain is imaginarily assumed to be *threo*-di-isotactic.

(3) The hydrogen bond is formed only when the conformation of two adjacent carboxyl groups is in *gauche*-staggered rotamers, as shown in Figure 4.

(4) When a certain conformation generated by the Monte Carlo attempt satisfies the requirements described above, the energy of hydrogen bond formation per a hydrogen bond,  $E_{HB}$ , is added to the total energy of the conformation,  $E_S$  in eq 4.

(5) Even when the hydrogen bond is formed, the electrostatic interaction between

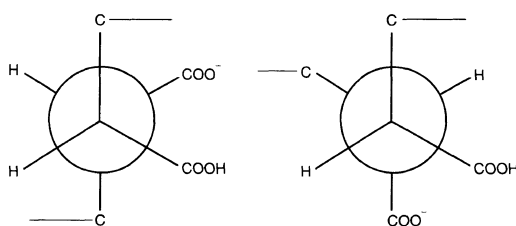


**Figure 4.** Newman's projections of monomer unit for the MA polyelectrolyte chains. C- and -C represent main chain. Both case can form hydrogen bond.

ionized beads is treated as the Debye-Hückel potential.

#### Calculated Quantities

At the end of every block of  $N^2$  motions, the mean-square end-to-end distance,  $\langle R^2 \rangle$ , and mean-square radius of gyration,  $\langle S^2 \rangle$ , and conformational energy of the polyion,  $\langle E \rangle$ , are calculated by following equations,

$$\langle R^2 \rangle = \langle (r_1 - r_N)^2 \rangle \quad (6)$$

$$\langle S^2 \rangle = \frac{1}{N} \left\langle \sum_{i=1}^N (r_i - r_{cm})^2 \right\rangle \quad (7)$$

$$\langle E \rangle = \frac{1}{N} \left\langle \sum_{i=1}^{N-1} \sum_{j=i+1}^N u_{ij} \right\rangle \quad (8)$$

where  $\langle \rangle$  denotes an ensemble average, and  $r_i$  is the position vector of  $i$ -th bead of chain,  $r_{cm}$  is a center of mass vector of the polymer chain. In the present paper, the energy of the conformation is represented by dividing  $\langle E \rangle$  by the thermal energy,  $kT$ . Unless otherwise noted, we refer the energy of conformation to  $\langle E \rangle / kT$ .

The computers used are Sun Microsystem/SunSPARC station IPC workstation and Nippon Data General/MV20000. A multiplicative congruential method is employed to operate the random number generators.

## RESULTS AND DISCUSSION

First, we examine the scaling relation for un-charged SAW chains on the three dimensional tetrahedral lattice to verify the accuracy

of the present program. In general, when the system is restricted to the non-branched lattice without the interaction, the scaling power between the chain dimension and bead number is 1.2, irrespective of the model used.<sup>1,2</sup> We confirm that the present simulation results precisely follow the scaling relation,  $\langle R^2 \rangle = aN^{1.2}$ , on tetrahedral lattice we simulate.

#### Monte Carlo Simulations without Hydrogen Bond

We investigate the conformational properties of the isolated PMA chains with the bead number, 10, 20, 40, 80, and 120. The hydrogen bond is not considered. The degree of dissociation ( $\alpha$ ) is varied from 0 to 1. The concentration of an added 1 : 1 electrolyte ( $C_s$ )

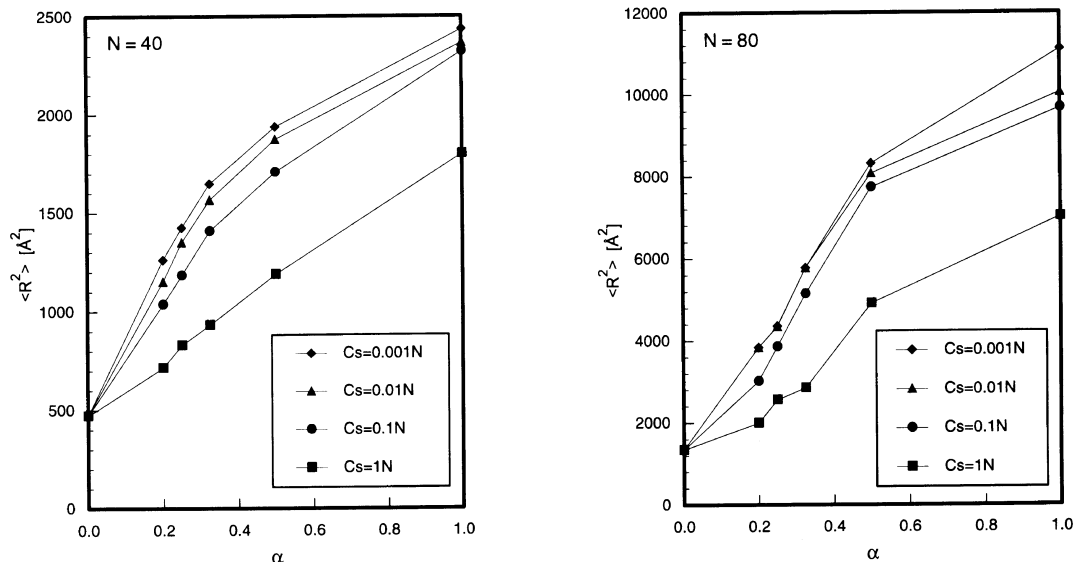


Figure 5. Plots of  $\langle R^2 \rangle$  against  $\alpha$  for PMA chain of  $N=40$  and  $80$  at various  $C_s$ .

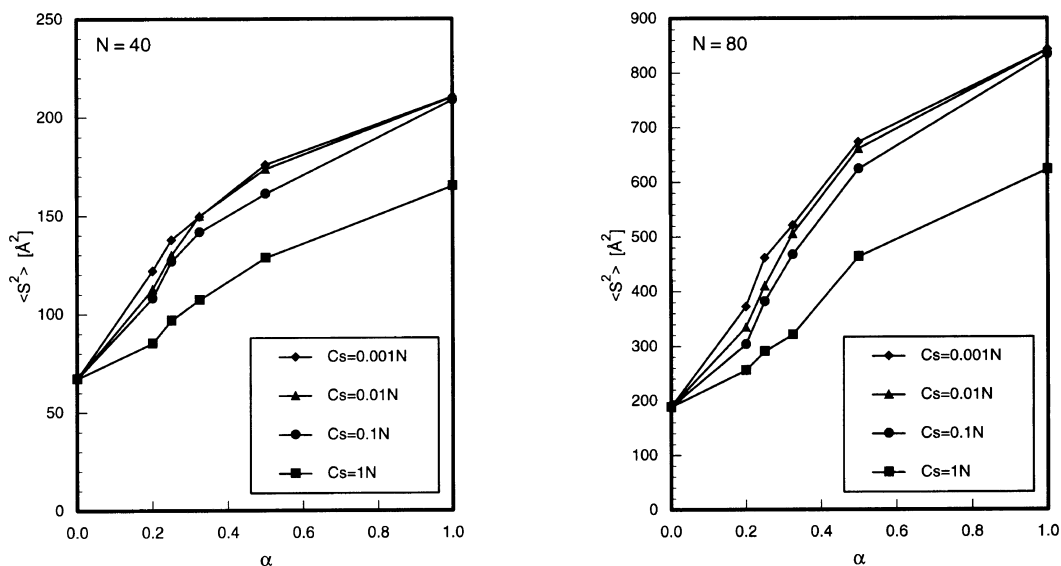


Figure 6. Plots of  $\langle S^2 \rangle$  against  $\alpha$  for PMA chain of  $N=40$  and  $80$  at various  $C_s$ .

is varied from 0.001 N to 1.0 N. In Figures 5 and 6,  $\langle R^2 \rangle$ , and  $\langle S^2 \rangle$  values simulated for  $N=40$  and 80 PMA chains at various  $C_s$  are plotted against  $\alpha$ . One can see in these figures that the chain dimension of PMA chain simulated increases monotonously with  $\alpha$  at any  $C_s$  and decreases with increasing  $C_s$  at constant  $\alpha$ . These are parallel to the viscosity behavior observed in the weak polyelectrolyte such as PAA.<sup>8</sup> The noteworthy feature in these figures is a  $C_s$ -dependence at constant charge density. In the region of  $C_s \leq 0.1$  N,  $C_s$ -dependence of  $\langle R^2 \rangle$  and  $\langle S^2 \rangle$  at constant  $\alpha$  is considerably weak. At  $C_s = 1.0$  N, the significant decreases of  $\langle S^2 \rangle$  and  $\langle R^2 \rangle$  are observed over whole  $\alpha$ . At  $C_s = 1.0$  N, the  $\kappa^{-1}$  (3.04 Å) is similar in magnitude to the charged bead separation at  $\alpha = 0.5$ , and the interaction between fixed charges are highly screened.

Experimentally, the linear dependence of  $[\eta]$  on  $C_s^{-1/2}$  at constant  $\alpha$  and  $N$  was observed in the solutions of the flexible polyelectrolytes having relatively low molecular weights.<sup>8</sup> In this case, the  $\langle S^2 \rangle$  is a linear function of  $C_s^{-1/3}$ . The simulated  $\langle S^2 \rangle$  and  $\langle R^2 \rangle$ , however, do

not follow  $C_s^{-1/3}$  at any  $\alpha$ . The similar simulation results for PAA chains have been reported by Hooper *et al.*<sup>18</sup> and Christos *et al.*<sup>20</sup> They observed the significant increase of persistence length with decreasing  $C_s$  in low  $C_s$ . According to Christos *et al.*, the addition of charges to a short chain increases the field exerted by the chain ends on the chain center and the stiffness of this central region.

At low  $\alpha$  (e.g.,  $\alpha = 0.2, 0.25$ ), the values of  $\langle R^2 \rangle$  and  $\langle S^2 \rangle$ , are a little scattered, because the number of the ionized beads is relatively small, resulting in the non-uniform arrangement of the ionized beads over the sampling space. In addition, for the simulation of a long chain ( $N > 120$ ) at high  $\alpha$ , the Monte Carlo simulation is very difficult, because the conformation energy converges very slowly, that is, a huge number of transitions is needed to attain an equilibrium conformation.

Figure 7 represents the dependence of conformational energy on  $\alpha$ . The value of  $\langle E \rangle / kT$  increases gradually with  $\alpha$  up to  $\alpha = 0.5$  and increases steeply above  $\alpha > 0.5$ . This dependence is similar to that of free energy calculated from integration of the potentio-

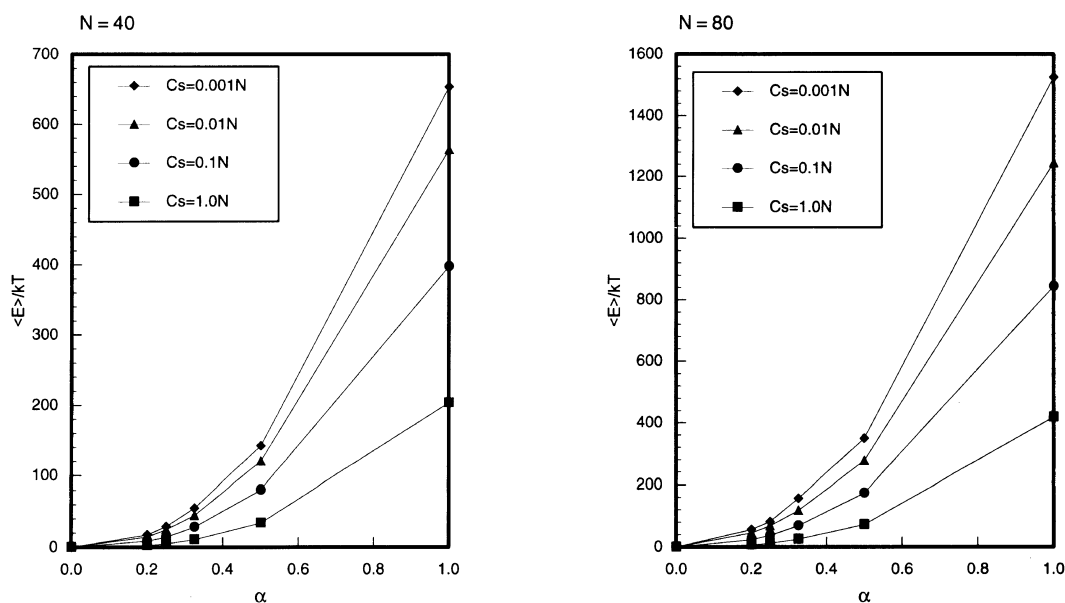
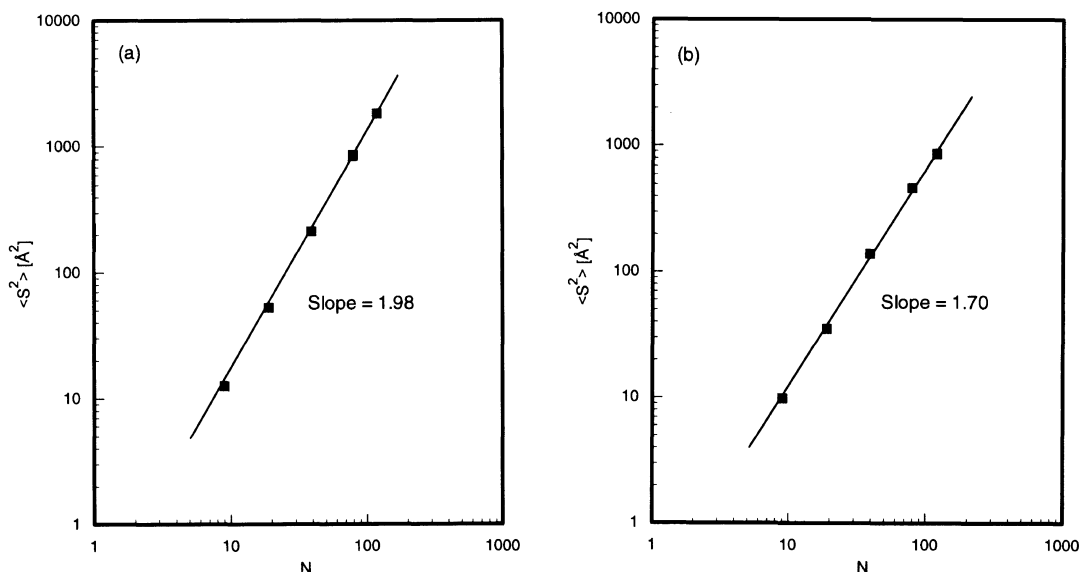


Figure 7. Plots of  $\langle E \rangle / kT$  vs.  $\alpha$  for PMA chain of  $N=40$  and 80 at various  $C_s$ .



**Figure 8.** Double logarithmic plots of  $\langle S^2 \rangle$  vs.  $N$  for PMA chain. (a)  $\alpha=1.0$  at  $C_s=0.01N$  and (b)  $\alpha=0.25$  at  $1.0N$ .

metric titration curves.<sup>11</sup>

In all instance,  $\langle R^2 \rangle$ , and  $\langle S^2 \rangle$ , can be expressed by a scaling relationship of the form

$$\langle J^2 \rangle = aN^b \quad (9)$$

where  $\langle J^2 \rangle = \langle R^2 \rangle$  or  $\langle S^2 \rangle$ , and  $a$  and  $b$  are constants dependent on the dimensionality and chain conformation. Figure 8 illustrates the scaling behavior of the polyions, *i.e.*, the plot of  $\log(N-1)$  vs.  $\log\langle S^2 \rangle$ , at  $\alpha=1.0$  and  $0.25$  at  $C_s=1.0N$  and  $0.01N$ . At  $\alpha=1.0$  and  $C_s=0.01N$ , the exponent  $b$  is 1.98, so that the conformation of the polyion is supposed to assume a rod-like conformation. At  $\alpha=0.25$  and  $C_s=1.0N$ , the exponent is 1.70, that is, the polyion chain approaches to a coil-like conformation but still assumes a largely expanded conformation. Thus, one concludes in the present simulations that the PMA polyion chain behaves as a semiflexible polymer in the intermediate region of  $\alpha$ .

In order to examine the conformation of the polyion in detail, the beads distribution function from center of mass of the polyion is calculated. Figure 9 represents the polyion beads distribution functions for  $N=80$  PMA

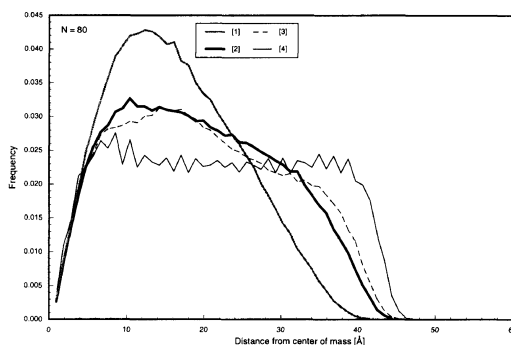


**Figure 9.** Distribution functions for the distance from the center of mass for PMA chain of  $N=80$ . (1)  $\alpha=0.25$  at  $C_s=1.0N$ , (2)  $\alpha=0.25$  at  $C_s=0.25N$ , (3)  $\alpha=0.5$  at  $C_s=1.0N$ , and (4)  $\alpha=0.5$  at  $C_s=0.25N$ .

chain at  $\alpha=0.5$  and  $0.25$ . The bead frequency at  $\alpha=0.5$  PMA chain at  $C_s=0.25$  is approximately independent of the distance from center of mass. This indicates that the conformation of polyion is nearly rod-like. The vibrations of the curve in this figure may be responsible for the incomplete averaging in the sampling cycles. On the other hand, at high  $C_s$  and low  $\alpha$ , the distribution of beads on polyion seems to be coil-like. Since the PMA chain at  $\alpha=0.5$  exactly corresponds to fully ionized



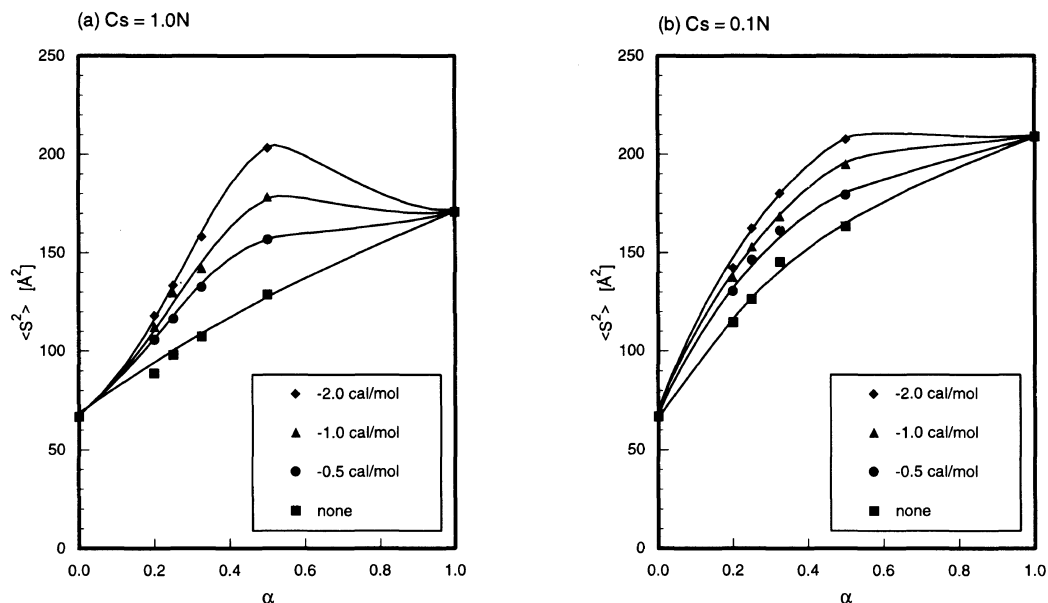


**Figure 10.** Plots of  $\langle S^2 \rangle$  against  $\alpha$  at various energies of hydrogen bond. (a)  $C_s = 1.0 N$  and (b)  $C_s = 0.1 N$ .

PAA chain, the complete ionized PMA chain assumes more rod-like conformation than PAA.

#### Monte Carlo Simulation with Hydrogen Bonding

The simulation results for the chain without hydrogen bond can explain qualitatively the experimental data of PAA in the salt solutions but not that of MA polyelectrolytes. It seems reasonably that such a simple simulation can not explain the characteristic viscosity behavior of MA polyelectrolytes. As a next step, one performs Monte Carlo simulation including the effect of hydrogen bond formation. Evidently, the intramolecular hydrogen bond is a short-range interaction. In this case, the polyion conformation can be determined by the balance between electrostatic repulsion and attraction force from hydrogen bond in short-range.

Figure 10 represents the dependence of energy of hydrogen bond ( $E_{HB}$ ) on PMA chain of  $N = 40$  at  $C_s = 1.0$  and  $0.10 N$ . Interestingly, at  $C_s = 1.0 N$  the  $\langle S^2 \rangle$  increases with  $\alpha$  up to  $\alpha = 0.5$ , attains maximum at  $\alpha = 0.5$ , and be-

yond it decreases noticeably. At  $C_s = 0.10 N$ , however, such a maximum point is not observed. In both  $C_s$ , the values of  $\langle S^2 \rangle$  in the region of  $0 < \alpha < 1$  increase with increasing  $E_{HB}$  assumed. Also, the greater the  $E_{HB}$ , the maximum at  $\alpha = 0.5$  appears more clearly. At  $C_s = 0.10 N$ , the electrostatic interaction is fairly strong to afford a rod-like conformation as described above. The additional hydrogen bond for the rod-like polyelectrolyte chain does not affect on the conformation. The simulation results explain qualitatively the experimental viscosity behavior of MA polyelectrolyte. We can conclude here that the characteristic viscosity behavior of the MA polyelectrolyte results from the competition between the electrostatic repulsion and the short-range attraction from hydrogen bond.

The counterion condensation phenomenon is not incorporated into the present model, as described before. The higher the charge density of the polyelectrolyte may be the greater the extent of counterions condensed. In fact, the dilute solution of PMA and PFA is found to exhibit a phase separation when neutralized with monovalent bases, prior to the complete

neutralization.<sup>2,3</sup> This is due to the strong counterion binding. The maximum point at  $\alpha=0.5$  seems to become more clearly by incorporating such counterion binding to the model. A further study is now in progress to consider this point.

## CONCLUSION

The conformational properties of MA polyelectrolyte chain are investigated by a mean of Monte Carlo simulation. The polyelectrolyte chains are modeled as a self-avoiding walk on tetrahedral lattice with charges fixed. Mean-square end-to-end distance,  $\langle R^2 \rangle$ , mean-square radius of gyration,  $\langle S^2 \rangle$ , and mean conformational energy,  $\langle E \rangle$ , are simulated as a function of degree of polymerization ( $N$ ), dissociation ( $\alpha$ ), and salt concentration ( $C_s$ ). The present simulation results provide an interpretation for characteristic viscometric behavior of MA polyelectrolytes which show a maximum in an intrinsic viscosity nearly at  $\alpha=0.5$ . The  $\langle S^2 \rangle$  in the region of  $\alpha < 0.5$  increases with energy of the hydrogen bonding assumed. The characteristic viscometric behavior of MA polyelectrolytes is concluded to result from the balance between repulsion from the electrostatic interaction and attraction from the hydrogen bonding in short-range.

*Acknowledgments.* The authors also thank Professor A. Minakata, Hamamatsu University School of Medicine for many helpful comments. The authors wish to thank the Toyohashi University of Technology Computer Center for generous use of computing facilities. This work was supported in a part by a Grant-in-Aid for the Encouragement of Young Scientists (No. 03750648) from the Ministry of Education, Science, and Culture of Japan.

## REFERENCES

1. H. Yamakawa, "Modern Theory of Polymer Solutions," Harper & Row, New York, N.Y., 1971.
2. P.-G. de Gennes, "Scaling Concepts in Polymer Physics," Cornell University Press, Ithaca, New York, N.Y., 1979.
3. F. Oosawa, "Polyelectrolytes," Marcel Dekker, New York, N.Y., 1971.
4. S. A. Rice and M. Nagasawa, "Polyelectrolyte Solution," Academic Press, New York, N.Y., 1961.
5. J. Skolnick and M. Fixman, *Macromolecules*, **10**, 944 (1977).
6. T. Odijk and A. C. Houwaart, *J. Polym. Sci., Polym. Phys. Ed.*, **16**, 627 (1978).
7. A. Katchalsky and S. Lifson, *J. Polym. Sci.*, **11**, 409 (1953).
8. I. Noda, T. Tsuge, and M. Nagasawa, *J. Phys. Chem.*, **74**, 711 (1970).
9. M. Nagasawa, "Molecular Conformation and Dynamics of Macromolecules in Condensed Systems," Elsevier, New York, N. Y., 1988.
10. J. Yamanaka, H. Matsuoka, N. Ise, S. Saeki, and M. Tsubokawa, *Macromolecules*, **24**, 3206 (1991).
11. (a) T. Kitano, S. Kawaguchi, K. Ito, and A. Minakata, *Macromolecules*, **20**, 1598 (1987). (b) T. Kitano, S. Kawaguchi, N. Anazawa, and A. Minakata, *Macromolecules*, **20**, 2498 (1987). (c) S. Kawaguchi, T. Kitano, K. Ito, and A. Minakata, *Macromolecules*, **23**, 731 (1990). (d) S. Kawaguchi, T. Kitano, and K. Ito, *Macromolecules*, **25**, 1294 (1992). (e) S. Kawaguchi, T. Kitano, and K. Ito, *Macromolecules*, **24**, 6030 (1991).
12. P. L. Dubin and U. P. Strauss, *J. Phys. Chem.*, **71**, 2757 (1967) and their subsequent papers.
13. N. Ohno, K. Nitta, S. Makino, and S. Sugai, *J. Polym. Sci., Polym. Phys. Ed.*, **11**, 413 (1973) and their subsequent papers.
14. G. S. Manning, *J. Chem. Phys.*, **51**, 924 (1969).
15. F. T. Wall, F. Mandel, and R. A. White, *J. Chem. Phys.*, **63**, 4393 (1975).
16. J. Dayantis and J.-F. Paliarne, *J. Chem. Phys.*, **95**, 6088 (1991).
17. C. Brender, M. Lax, and S. Windwer, *J. Chem. Phys.*, **74**, 2526 (1981).
18. H. H. Hooper, H. W. Blanch, and J. M. Prausnitz, *Macromolecules*, **23**, 4820 (1990).
19. G. A. Christos, S. L. Carnie, and T. P. Creamer, *J. Chem. Phys.*, **89**, 6484 (1988).
20. G. A. Christos and S. L. Carnie, *J. Chem. Phys.*, **92**, 7661 (1990).
21. N. Metropolis, A. W. Rosenbluth, M. N. Rosenbluth, A. T. Teller, and E. Teller, *J. Chem. Phys.*, **21**, 1087 (1953).
22. G. A. Christos and S. L. Carnie, *J. Chem. Phys.*, **91**, 439 (1989).
23. S. Kawaguchi, S. Toui, M. Onodera, K. Ito, and A. Minakata, *Macromolecules*, **26**, 3081 (1993).